

09.2;11.3;14

Optical magnetometric sensor for magnetoencephalographic complexes

© A.K. Vershovskii, M.V. Petrenko

Ioffe Institute, St. Petersburg, Russia

E-mail: antver@mail.ioffe.ru

Received September 28, 2022

Revised January 16, 2023

Accepted January 16, 2023

A new implementation of the method of optical pumping of alkaline atoms in the scheme of a highly sensitive compact single-beam sensor of a nonzero magnetic field is proposed, which allows it to be used as part of a magnetoencephalographic complex with a remote laser pumping source. The proposed method makes it possible, in particular, to pump an array of sensors with a single source of polarization-modulated resonant radiation connected to sensors by means of polarization-supporting optical fibers. A model experiment has been carried out confirming the principle feasibility and effectiveness of the method.

Keywords: Optically detectable magnetic resonance, quantum magnetometer, magnetoencephalography.

DOI: 10.21883/TPL.2023.03.55693.19378

The past decade was characterized by an upsurge in interest in magnetic methods of examination of ultra-weak magnetic fields in the brain (magnetoencephalography, MEG). This upsurge is mostly attributable to the introduction of compact optical magnetic field (MF) sensors based on the magnetic resonance (MR) effect [1–6], which are competitive in their metrological characteristics with high-priced stationary superconducting SQUID systems [7]. The development of the first optical SERF sensors [1], which remain operational only in „zero“ fields (i.e., magnetically isolated chambers), coincided with the onset of the search for ways to produce more compact nonzero-field sensors without sacrificing their sensitivity. Such sensors should allow one to lower dramatically the requirements as to suppression of the external MF and its spatial gradients [6,8,9]. Specifically, a nonzero-field sensor based on alkaline atoms has been proposed in our earlier study [10]. This design satisfies MEG requirements in all the key parameters (sensitivity, speed, and the ability to function without inducing radio frequency interference that affects the operation of adjacent sensors) while remaining extremely simple and compact. These advantages of the proposed sensor stem from the fact that a single beam with its ellipticity varying in time (from left-handed elliptical polarization to a linear one and further to right-handed elliptical polarization) is used for pumping and MR detection. The frequency of this beam is tuned in resonance with transitions from hyperfine level $F = I - 1/2$ of the $S_{1/2}$ ground state to nearby excited levels $F = I \pm 1/2$ of the closest $P_{1/2}$ excited state (two short-wave components of the D_1 line of an alkaline metal) [11,12]. The circular radiation component modulated at the MR frequency (Larmor frequency) is used for optical pumping of atomic magnetic moments (the so-called Bell–Bloom scheme [13]), while MR detection is performed at the $F = I + 1/2$, $m_F = F \leftrightarrow F - 1$ ground-state transition by monitoring the rotation of the angle of polarization of the linearly polarized radiation component at

the Larmor frequency (the so-called M_X scheme). Various single-beam schemes proposed earlier (see, e.g., [14–16]) simplified the design at the tradeoff of a reduced sensitivity (e.g., by combining pumping and detection beams into one beam with certain average parameters). In [10], the processes of pumping and detection are separated in time and correspond to different precession phases; the beam parameters remain optimum (tailored to the current process) at all times, and the efficiency of both process is thus maximized.

As was noted in [10], the proposed scheme has a major disadvantage: it is hard to transmit radiation with modulated ellipticity along a fiber line. This disadvantage becomes especially significant in MEG complexes, where a single high-power laser is used for optical pumping of an array of sensors with radiation transmitted to each of them along a designated fiber line (it should be noted here that a considerable (several milliwatts or even several tens of milliwatts) radiation power is normally required to reach the needed sensitivity of nonzero-field sensors based on cells with alkaline atoms and a buffer gas; thus, these devices cannot be integrated with low-power VCSELs, differing in this respect from zero-field SERF sensors [17]). The use of a common pumping source allows for considerable simplification of the design and makes it possible to reduce the device cost and suppress technical noise due to subtraction of the common pumping noise.

In the present study, we propose to use a standard single-mode polarization-maintaining (SM-PM) optical fiber in the scheme discussed above to transmit linearly polarized radiation matching the eigen modes of this fiber. A PM fiber has two modes of this kind characterized by orthogonal (s and p) polarizations propagating along the fiber axes. The phase delay between modes is undetermined, thus precluding one from transmitting radiation with elliptical polarization. Therefore, we propose to use an SM-PM fiber to transmit fully linearly polarized radiation with its

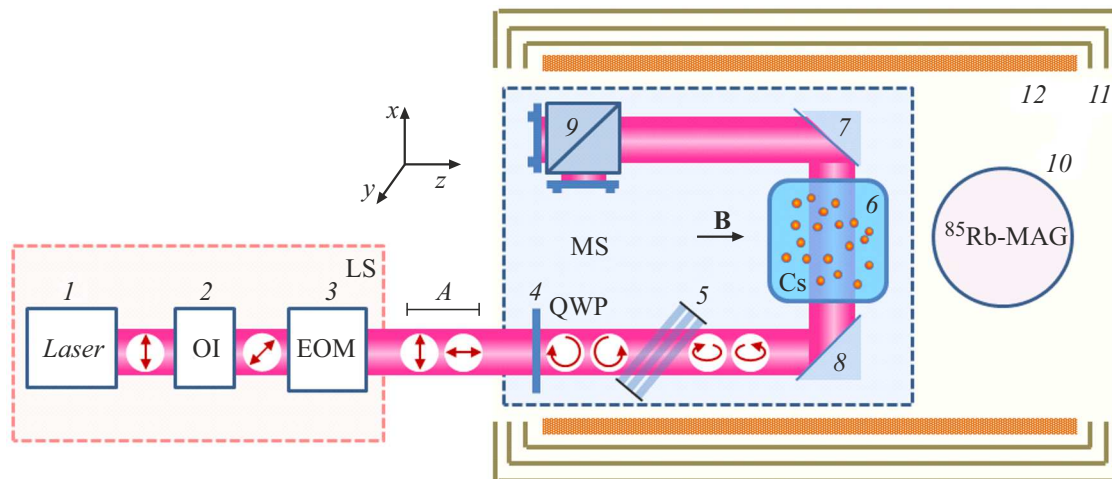


Figure 1. Simplified diagram of the experiment. LS is the light source and MS is the model of a magnetometric sensor. 1 — Laser, 2 — optical isolator (OI), 3 — electro-optical modulator (EOM), 4 — quarter-wave plate (QWP), 5 — tunable linear polarizer, 6 — gas cell with Cs vapor, 7 and 8 — mirrors, 9 — balanced photodetector, 10 — ^{85}Rb -based magnetometer (MAG), 11 — magnetic shield, 12 — solenoid, A — section within which light may be transmitted along a fiber line. Arrows denote the polarization states of a beam corresponding (after EOM) to two modulation half-periods.

polarization azimuth modulated with a duty ratio of 50%: p polarization is transmitted within one half-period of the Larmor frequency, while s polarization occupies the other half-period. A quarter-wave plate (QWP) with its axes positioned at an angle of 45° to the fiber axes is mounted at the fiber output and converts these two polarizations into circular ones (left- and right-handed, respectively). A tunable linear polarizer (e.g., an inclined semi-transparent mirror or a stack of glass plates, which is often referred to as a Stoletov pile) is positioned behind the QWP and converts circular polarization into an elliptical one. A linear component needed for detection then emerges in transmitted radiation, and the direction of polarization of this component is specified exclusively by the polarizer orientation.

The difference in characteristics of radiation between the proposed scheme and the one discussed in [10] boils down to the following: the ellipticity is modulated in accordance with a rectangular time law instead of a sinusoidal one. Therefore, both circular and linear components are present in radiation at all times and are characterized by a constant intensity; earlier, we have regarded this as a compromise that may lead to degradation of device parameters. The influence of shape of modulation in the common two-beam Bell–Bloom scheme has been examined in [18]. It has been demonstrated that rectangular modulation induces slight broadening of the MR signal, but still allows one to achieve similar values of the ultimate sensitivity. However, it needs to be verified whether the same is true for the single-beam scheme. Therefore, we simulated the corresponding pumping conditions and examined the MR parameters.

The measurement setup used in the present study was characterized in [10,18]; in essence, this setup is a magnetometric sensor model with an external pumping source

that are introduced into an MF stabilizer. A cubic cell $8 \times 8 \times 8$ mm in size contained saturated cesium vapor and nitrogen under a pressure of ~ 100 Torr and was positioned in the central area of a multilayer magnetic shield with an MF induction of $\sim 12 \mu\text{T}$ maintained within it by an active stabilization circuit. The ^{85}Rb isotope served as an active magnetometer element providing MF stabilization. This helped suppress the unwanted influence of a radio-frequency field produced by the magnetometer on Cs atoms. The sensor model (see Fig. 1) also featured a quarter-wave plate and a tunable linear polarizer (a stack of $N = 1-12$ Brewster-angled glass plane-parallel plates) that allowed us to minimize attenuation of the chosen linear polarization.

The results of measurements are shown in Fig. 2. It follows from the comparison of MR parameters with those presented in [10] that the proposed modification of the Bell–Bloom scheme does not trigger any significant degradation of its parameters. Specifically, the ultimate short-term sensitivity estimated by the ratio of the amplitude of the resonance to its width and the spectral density of shot noise of the photocurrent is $\sim 11 \text{ fT}/\sqrt{\text{Hz}}$ at an operation speed on the order of $\Gamma/(2\pi) = 500$ Hz. The results presented in [19] verify the applicability of the discussed scheme in MEG complexes. It was demonstrated in this study that the projected accuracy of localization of individual neuronal dipoles ($\sim 10 \text{ nA} \cdot \text{m}$) is on the order of 1 cm for an array of 128 scalar optical sensors with a sensitivity of $70 \text{ fT}/\sqrt{\text{Hz}}$ and a band width of 100 Hz in the case of averaging over 100 records. The accuracy may be raised to 1 mm in the same conditions if the sensitivity of sensors reaches $7-10 \text{ fT}/\sqrt{\text{Hz}}$.

The operation speed of the setup is specified by the MR half-width and may be increased additionally by raising the temperature of the working cell (with a simultaneous

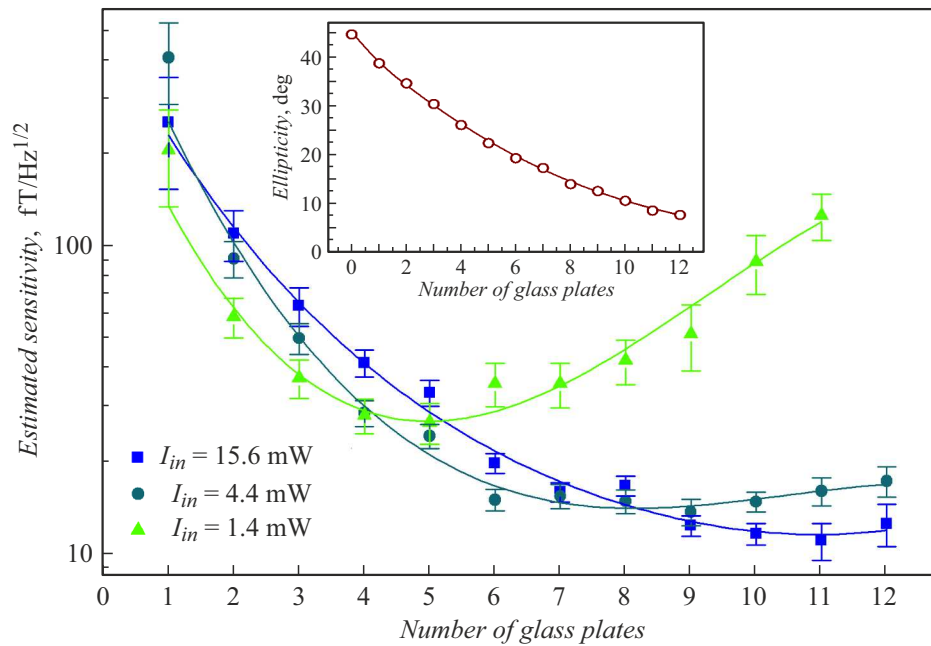


Figure 2. Dependences of estimated ultimate (limited by shot noise) sensitivity values for three input intensities I_{in} on the number of glass plates in a Stoletov pile. Curves were plotted for better readability. The dependence of the beam ellipticity on the number of plates in a Stoletov pile is shown in the inset.

enhancement of the optical pumping power). The MR width also defines the allowed MF nonuniformity (i.e., the maximum difference between MF values at sites where individual sensors are located).

The optimum sensitivity is achieved at an ellipticity of $\sim 10.5^\circ$. This corresponds to a relative intensity of 36% of the circularly polarized component and agrees fully with the data from [10].

The linear polarizer in our experiment was positioned so that electric vector \mathbf{E} of the linear radiation component was parallel to MF vector \mathbf{B} ; with pumping by the D_1 line, this makes it possible to minimize the MR broadening by the linear radiation component (avoid its destructive interaction with levels $F = I + 1/2$, $m_F = \pm F$ that are populated the most in the process of optical pumping). When a sensor is rotated about its axis, which goes through the cell center in the direction of light propagation (along axis x in Fig. 1), the parallel alignment of vectors \mathbf{E} and \mathbf{B} may be established by choosing the right direction of the polarizer axis. This should allow one to rotate a sensor by 360° about its axis while maintaining the operating parameters and serves as an additional advantage of the proposed scheme.

Thus, it was demonstrated that the design of a compact single-beam sensor for magnetoencephalographic complexes, which was proposed in our earlier study, may be modified to exclude the transmission of elliptically polarized radiation from a pumping source to the sensor. This provides an opportunity to use a single-mode fiber for transmission of radiation from a remote laser pumping source, thus eliminating the last conceptual obstacle on the

path to a nonzero-field magnetoencephalographic system based on single-beam optical sensors.

Conflict of interest

The authors declare that they have no conflict of interest.

References

- [1] I.K. Kominis, T.W. Kornack, J.C. Allred, M.V. Romalis, *Nature*, **422** (6932), 596 (2003). DOI: 10.1038/nature01484
- [2] J. Iivanainen, M. Stenroos, L. Parkkonen, *NeuroImage*, **147**, 542 (2017). DOI: 10.1016/j.neuroimage.2016.12.048
- [3] E. Boto, S.S. Meyer, V. Shah, O. Alem, S. Knappe, P. Kruger, T.M. Fromhold, M. Lim, P.M. Glover, P.G. Morris, R. Bowtell, G.R. Barnes, M.J. Brookes, *NeuroImage*, **149**, 404 (2017). DOI: 10.1016/j.neuroimage.2017.01.034
- [4] K.-M.C. Fu, G.Z. Iwata, A. Wickenbrock, D. Budker, *AVS Quantum Sci.*, **2** (4), 044702 (2020). DOI: 10.1116/5.0025186
- [5] N.V. Nardelli, A.R. Perry, S.P. Krzyzewski, S.A. Knappe, *EPJ Quantum Technol.*, **7** (1), 11 (2020). DOI: 10.1140/epjqt/s40507-020-00086-4
- [6] M.E. Limes, E.L. Foley, T.W. Kornack, S. Caliga, S. McBride, A. Braun, W. Lee, V.G. Lucivero, M.V. Romalis, *Phys. Rev. Appl.*, **14** (1), 011002 (2020). DOI: 10.1103/PhysRevApplied.14.011002
- [7] D. Cohen, *Science*, **175** (4022), 664 (1972). DOI: 10.1126/science.175.4022.664
- [8] R. Zhang, W. Xiao, Y. Ding, Y. Feng, X. Peng, L. Shen, C. Sun, T. Wu, Y. Wu, Y. Yang, Z. Zheng, X. Zhang, J. Chen, H. Guo, *Sci. Adv.*, **6** (24), eaba8792 (2020). DOI: 10.1126/sciadv.aba8792

- [9] Y. Guo, S. Wan, X. Sun, J. Qin, *Appl. Opt.*, **58** (4), 734 (2019). DOI: 10.1364/AO.58.000734
- [10] M.V. Petrenko, A.S. Pazgalev, A.K. Vershovskii, *Phys. Rev. Appl.*, **15** (6), 064072 (2021). DOI: 10.1103/PhysRevApplied.15.064072
- [11] T. Scholtes, V. Schultze, R. IJsselsteijn, S. Woetzel, H.-G. Eyer, *Phys. Rev. A*, **84** (4), 043416 (2011). DOI: 10.1103/PhysRevA.84.043416
- [12] E.N. Popov, V.A. Bobrikova, S.P. Voskoboinikov, K.A. Barantsev, S.M. Ustinov, A.N. Litvinov, A.K. Vershovskii, S.P. Dmitriev, V.A. Kartoshkin, A.S. Pazgalev, M.V. Petrenko, *JETP Lett.*, **108** (8), 513 (2018). DOI: 10.1134/S0021364018200122.
- [13] W.E. Bell, A.L. Bloom, *Phys. Rev. Lett.*, **6** (6), 280 (1961). DOI: 10.1103/PhysRevLett.6.280
- [14] V. Schultze, B. Schillig, R. IJsselsteijn, T. Scholtes, S. Woetzel, R. Stolz, *Sensors*, **17** (3), 561 (2017). DOI: 10.3390/s17030561
- [15] A.L. Bloom, *Appl. Opt.*, **1** (1), 61 (1962). DOI: 10.1364/AO.1.000061
- [16] S. Groeger, G. Bison, J.-L. Schenker, R. Wynands, A. Weis, *Eur. Phys. J. D*, **38** (2), 239 (2006). DOI: 10.1140/epjd/e2006-00037-y
- [17] J. Iivanainen, R. Zetter, L. Parkkonen, *Hum. Brain Mapp.*, **41** (1), 150 (2020). DOI: 10.1002/hbm.24795
- [18] A.K. Vershovskii, M.V. Petrenko, *Tech. Phys.*, **66**, 821 (2021). DOI: 10.1134/S106378422105025X.
- [19] R.J. Clancy, V. Gerginov, O. Alem, S. Becker, S. Knappe, *Phys. Med. Biol.*, **66** (17), 175030 (2021). DOI: 10.1088/1361-6560/ac18fb